Modelling fluid and particulate flow through a ventriculoperitoneal shunt in a variable temperature environment

Tshiamo Ramokoka[1], and *Muaaz* Bhamjee[1,*]

[1]Department of Mechanical Engineering Science, Faculty of Engineering and the Built Environment, University of Johannesburg, Auckland Park Kingsway Campus, Johannesburg, South Africa

Abstract. One of the most prevalent causes of failure for a ventriculoperitoneal shunt is blockage, the other being infection. This study looks at the blockage of the shunt valve, and whether the occlusion of a shunt valve is accelerated by the presence of an infection. This study assumes that an infection will raise the number of white blood cells contained in the cerebrospinal fluid to fight it and will thus accelerate shunt occlusion. The experiment simulates a shunt system by suspending a shunt valve in a water bath that has a temperature that varies between 37℃ and 41℃. A computational fluid dynamics model of the shunt system is used to gain further insight into the flow behaviour under these conditions. The results of the CFD model were validated using the experimental results. There was an average error of 15% between the readings that were obtained in the experiment and the CFD model. The experimental results showed that there was a decrease in the volume flow rate at the outlet of the shunt system, which was not large enough to point towards any blockage. Both the model predictions and the experimental results show that increased temperature and particulate concentration alone do not result in shunt occlusion, particularly at the shunt valve. This result effectively excluded the shunt valve as a region of shunt occlusion due to infection, as an infection occurs due to the growth of bacteria along the surfaces of the shunt system and this bacterial growth is more likely to occur at the proximal and distal ends of the shunt system.

Nomenclature

C_D	-	drag coefficient	μ	-	Dynamic viscosity (kg/(m.s))
C_{vm}	-	virtual mass coefficient	υ	-	kinematic viscosity (m^2/s)
d_p	-	diameter of particulate	p	-	Pressure (Pa)
d_{ij}	-	deformation tensor	ρ	-	Density (kg/m^3)
$D_{T,p}$	-	thermophoretic coefficient	Re	-	Reynolds number

* Corresponding author: muaazb@uj.ac.za

E	-	energy (J)	T	-	Temperature (°C, K)
$\bar{F}$	-	force (N)	$\bar{\bar{\tau}}_{eff}$	-	Shear stress (Pa)
g	-	gravitational acceleration (m/s^2)	$\vec{v}$	-	Fluid velocity (m/s)
h	-	sensible enthalpy of fluid (J/kg)	$\boldsymbol{u}_p$	-	Particle velocity (m/s)
$\bar{I}$	-	unity tensor	m_p	-	Particle mass (kg)
k_{eff}	-	Effective conductivity	ρ_p	-	Particle density (kg/ m^3)

1 Introduction

A ventriculoperitoneal (VP) shunt is used in the treatment of hydrocephalus, a medical condition caused by the inadequate drainage of cerebrospinal fluid (CSF) from the ventricles [1]. The rate at which the CSF is absorbed is less than that at which the CSF is produced, which results in the accumulation of CSF in the ventricles [1]. The treatment of hydrocephalus by the insertion of a VP shunt is one of the more common treatment methods for hydrocephalus [2]. A VP shunt comprises of three elements: an inflow/ventricular catheter, a valve for unidirectional flow and a peritoneal/outflow catheter [3]. The inflow catheter drains the excess CSF from the ventricles; the valve controls the flow of the CSF through the shunt system and the peritoneal catheter routes the CSF from the valve to the peritoneal cavity, where it is then absorbed [3].

The shunt system can fail in many ways, such as through over-drainage, underdrainage, infection, blockage, leaks, migration, and discontinuity [3], [4]. Unlike the other methods of shunt failure, infection is a non-mechanical problem, as infection is typically caused by the growth of bacteria along parts of the shunt system [5]. Particulates contained in the CSF (i.e., brain tissue, proteins, blood cells) can create a blockage in the shunt system, depending on the concentration of the particulates. An infection will result in an increase of the temperature of the CSF, as well as the amount of white blood cells contained in the CSF. This will increase the likelihood of a blockage occurring in the shunt system.

A CSF analysis is usually done to confirm an infection. A positive CSF analysis will show an increase in the number of white blood cells present ($1000 - 5000\ cells/mcL$) with a high percentage of neutrophils ($> 80\%$), as well as an increased protein concentration [6]. Per Tamburrini, Calderelli and Di Rocco [7], infection is the second most prevalent type of shunt failure in children, second to mechanical failure. Fever is typically a sign of bacterial infection but can be mild or there could be no fever present, which may delay the diagnosis [7].

Studies of CSF shunt failures in children were looked at to determine how prevalent shunt failures due to infection are, as well as to how prevalent reoccurrences of shunt infections are in children. The study by Simon et.al. [8] did a statistical analysis of shunt revisions in children over a four-year period and it was determined that the risk of infection can be attributed to the revision of a CSF shunt. Moreover, it was found that the risk of infection increases with an increase in the number of shunt revisions a patient had, with the risk being 13 times greater in patients who have had 2 or more revisions than those who have had no revisions [8].

A study was conducted in Turkey which was centred around determining the rate of recurring shunt infections after the initial shunt infection has been treated [9]. The study was done over 10 years [9]. For this study, the recovery of 428 patients was tracked [9]. Of these patients, 58 were treated for an infection [9]. The final findings of the study detail a method of effectively reducing the risk of recurring shunt infections. In the case of infection, the total removal of the shunt and insertion of a new external ventricular drainage catheter should be

used to treat the infection [9]. In addition, isolating the pathogen responsible for the infection and using antibiotics appropriately will decrease the length of the infection [9].

A study was conducted at the University of Johannesburg in 2017, which looked at the flow of fluid and particulates through a VP shunt [10]. The shunt valve was the point of interest, as it was assumed that the blockage was likely to occur at this region [10]. The only drawback from this study was that the effects of the change in fluid temperature were not studied.

The literature has not completely addressed how a change in the temperature of the CSF (which is a simulation of infection through the symptom that is fever), as well as a change in the concentration of the particulates in the CSF will affect the behaviour of the VP shunt system. This is of interest particularly where such changes in temperature, and subsequent increase in the concentration of particulates, will affect the potential likelihood of the occurrence of a blockage in the shunt system. Thus, the aim of this study is to investigate the flow characteristics of CSF containing particulates through the VP shunt, while the temperature of the CSF is not kept constant. The methodology used for this study include using an experimental test bench to study the flow of the fluid and particulates through a VP shunt, as well as setting up a computational fluid dynamics (CFD) model for studying the flow through the VP shunt. The results of the CFD model will be validated against those of the experiment. This study is only limited to paediatric cases.

2 CFD Model

2.1 Geometry and computational mesh

The geometry of the shunt valve was derived from that of the Medtronic CSF Control Valve, which was used in the experiment. The geometry for the model was modified slightly but has the general shape of the Medtronic shunt valve. Fig. **1** shows the geometry of the CSF Control Valve.

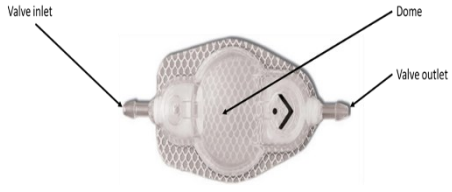

Fig. 1. CSF Control Valve geometry

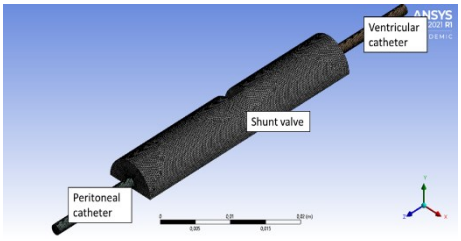

Fig. 2. Mesh

To simplify the model, the shunt valve was drawn as a cylinder cut in half to serve as the dome shaped chamber. A void was introduced into the geometry to model the flow restriction created by the valve which only opens when the differential pressure is enough to drive the fluid through the shunt valve. The dimensions for the model were directly derived from those of the Delta Valve produced by Medtronic [11]. The dimensions were used because the CSF Control Valve and the Delta Valve are very similar in appearance. The diameter of the inlet and outlet catheters was set at 1.5mm, the length of the ventricular and peritoneal catheters was set at 15mm and the length of the shunt valve was set at 14mm. The radius of the hemispherical shape of the valve was set at 4mm.

The mesh comprises of a mixture of tetrahedral and hexahedral cells. The tetrahedral cells were converted to polyhedra to improve the cell quality, as well as reduce cell count and decreases computational power [12]. The element order was selected to be quadratic. Fig. 2 shows the mesh that was created for this model.

A mesh convergence study to ensure that the results were mesh independent [13]. A method presented by Roache was used for the mesh convergence study, which is based on the Richardson Extrapolation [14]. The Richardson Extrapolation, and thus the Grid Convergence Index (GCI), work on the basis that the solution from each grid is within the asymptotic range (GCI ≈ 1) [14]. Three meshes of element sizes that differed by a grid refinement ratio of $r = 1.41$ were developed. For the mesh independence study, three meshes were generated, for element sizes $0.5mm$, $0.354mm$ and $0.25mm$. The models were run and the results for each of these meshes used to find the Grid Convergence Index for the fine grid [14]. The GCI was found to be 1.004, which shows that the fine grid (0.25mm) is in the asymptotic range, and thus, the solution is mesh independent. Therefore, the element size used in all subsequent models is $0.25mm$.

2.2 Governing equations

The flow through the shunt system was modelled as steady incompressible flow, as the velocity of the fluid/particulate mixture is quite low, which will result in a Mach number less than 1. Laminar flow was selected for this CFD model as the typical flow of CSF has a Reynolds number that is less than 10 [15]. The flow of fluid through the shunt system is governed by the conservation of mass and conservation of momentum equations [16] as per equations (1) and (2) respectively.

$$\nabla \cdot (\rho \vec{v}) = 0 \tag{1}$$

For a compressible Newtonian fluid, the Navier-Stokes equations are [17]:

$$\rho \vec{v} \cdot \nabla \vec{v} = -\nabla p + \nabla \cdot \left(\mu(\nabla \vec{v} + (\nabla \vec{v})^T) - \frac{2}{3}\mu\left(\nabla \cdot \vec{v}\right)\bar{I} \right) + \bar{F} \tag{2}$$

The force $\bar{F}$ accounts for source terms such as body forces (due to gravity) as well as momentum exchange from the particulate to the fluid. The energy equation solved by ANSYS Fluent encompasses the transfer of energy due to conduction and viscous dissipation [18]. The equation is written as follows:

$$\vec{v}(\rho E + p) = \nabla \cdot \left[k_{eff} \nabla T + \left(\bar{\bar{\tau}}_{eff} \cdot \vec{v} \right) \right] \tag{3}$$

Due to the temperature gradient between the surroundings and the fluid flowing through the VP shunt system, heat transfer will occur through the walls of the shunt system. The term E in equation (3) can be written as:

$$E = h - \frac{p}{\rho} + \frac{v^2}{2} \tag{4}$$

The *Discrete Particulate Modelling (DPM)* model was selected, to introduce particulates into the VP shunt system. The particulates contained in the CSF are protein, monocytes, and lymphocytes. The lymphocytes and the monocytes have a diameter of $14\mu m$ and $20\mu m$ respectively [19]. The protein cells have a diameter of $3.8nm$ [20].

The physical models that were selected for the DPM were the Drag Force, Virtual Mass Force, Pressure Gradient Force, Saffman Lift Force, and the Thermophoretic Force. The ratio of the density of the fluid to that of the particulate is greater than 0.1, therefore the Pressure Gradient Force and the Virtual Mass Force have a significant effect on the results of the CFD model [18]. The Saffman Lift Force was enabled as it is the force that results from shear and

the Thermophoretic Force was enabled to account for the effect of fluid temperature gradients on the particulates [18]. A key assumption that was made was that the particulates have a spherical shape. Thus, the particle force balance is given by [18]:

$$m_p \frac{d\boldsymbol{u_p}}{dt} = \frac{18\mu}{\rho_p {d_p}^2}\frac{C_D Re}{24}(\vec{v} - u_p) + C_{vm}\frac{\rho}{\rho_p}\left(\boldsymbol{u}_p\nabla\vec{v} - \frac{d\boldsymbol{u_p}}{dt}\right) + m_p\frac{\rho}{\rho_p}(\vec{v}\nabla\vec{v}) + m_p\frac{2(2.594)\nu^{\frac{1}{2}}\rho d_{ij}}{\rho_p d_p(d_{lk}d_{kl})}\left(\vec{v} - \boldsymbol{u}_p\right) + \mathrm{D_{T,p}}\frac{1}{T}\nabla T + m_p\boldsymbol{g}\frac{(\boldsymbol{\rho_p}-\boldsymbol{\rho})}{\boldsymbol{\rho_p}} \quad (5)$$

The fluid is assumed to be Newtonian despite the presence of the monocytes, lymphocytes and albumin. The white blood cells (monocytes and lymphocytes) are solids contained in the blood plasma as well as the CSF and, thus, are insoluble. Therefore, they arguably will not affect the viscosity of the CSF, thus, maintaining the Newtonian assumption [21]. However, proteins (albumin) are soluble and will have an impact on the fluid viscosity and violate the Newtonian assumption [21], [22]. In future work a non-Newtonian model will be incorporated to account for impact of the proteins on the CSF viscosity and the viscoelasticity of the blood plasma akin to [23], [24]. To account for the effect of the particles on the fluid a two-way coupling was implemented between the fluid phase and particulates. However, the effect of the particulates on the fluid phase is only via momentum transfer as per equations (2).

This study assumes that an infection will raise the number of white blood cells contained in the cerebrospinal fluid. The white blood cells were modelled as particulates. Thus, in this study the model reduces the biological complexity involved in the process of infection to a.) the change in temperature of the CSF and/or shunt surfaces and b.) an increase in particulates as a consequence of the rise in white blood cells in response to infection. Thus, the biological complexity is reduced to heat transfer and particulate mechanics.

2.3 Material properties

The materials used in this CFD model include water, medical grade silicone and brain matter. The water is representative of the CSF, as they have similar properties [21], [25]. The medical grade silicon is the material used for the components of the shunt system and the brain matter is composed of blood cells and protein. The thermophysical properties for these materials are given in Table 1 [19], [20], [26], [27], [28].

Table 1. Thermophysical properties

Cell type	Density (kg/m^3)	Dynamic viscosity (kg/(m.s))	Enthalpy (J/kg)	Thermal conductivity (W/m.K)	Specific heat capacity (J/kg.°C)
Lymphocyte	1077	-	-	-	-
Monocyte	1077	-	-	-	-
Albumin	0.15	-	-	-	-
Silicone	2300	-	-	0.2	1050
Water	998.2	0.1003	154950	0.598	4200

2.4 Boundary conditions

Fig. **3** shows an image of the boundary conditions for the CFD model. The two primary locations for the boundary conditions are the inlet and outlet of the shunt system. The inlet and outlet of the shunt valve are points of interest because any changes in the flow characteristics can be observed at these locations. A constant temperature condition ($37°C$, $38°C$, $39°C$, $40°C$ or $41°C$) was placed on the walls of the shunt system to model the heat transfer between the shunt system and the surroundings. The boundary conditions for the CFD model are summarised in Table 2.

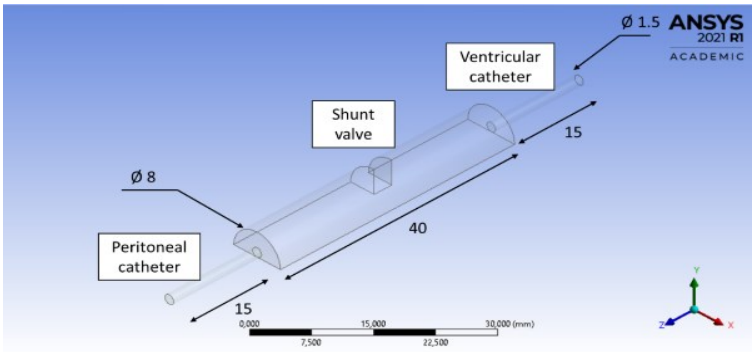

Fig. 3. Boundary conditions

Table 2. Boundary conditions

Boundary	Type	Velocity (m/s)	Pressure (Pa)	Temperature (°C)	DPM type
Inlet	Velocity inlet	0,01572	0	37	Reflect
Outlet	Pressure outlet	-	0	Solution dependent	Escape
Ventricular catheter	Wall	-	-	Constant Temperature	Reflect
Shunt valve	Wall	-	-	varies	Trap
Peritoneal catheter	Wall	-	-	varies	Reflect

When shunt blockage occurs there are also upstream changes that occur, thus, the upstream velocity profile may not be constant. However, a constant velocity profile is used in the models in this study so that we could compare the model predictions directly to the experimental results. In the experimental setup a syringe pump was used to mimic the upstream/inlet flow condition. Whilst not fully representative of the non-constant upstream condition in 'reality', it was representative of the experimental setup against which the CFD predictions were validated.

2.5 Solver settings

The pressure-velocity coupling that was selected is the SIMPLE coupling. The discretization selected for the gradient was "Least Squares Cell-Based". The pressure discretization scheme was "standard". The discretization scheme selected for momentum and energy was "Second Order Upwind". The model was solved as a steady state problem. The

tracking scheme used for the DPM is the Runge-Kutta scheme and the source terms were linearised to increase numerical stability for steady-state flows.

3 Experimental Setup and Results

3.1 Experimental setup

The aim of the experiment was to determine whether an increase in temperature and particulate concentration would lead to shunt occlusion. The test bench was set up as per Fig. **4** and the volume to be infused (VTBI) for the syringe pump was set at $100ml/hr$, as the normal flow rate of CSF at $20ml/hr$ was too low to yield meaningful results. The concentration of the particulates/gelatine powder varied between $3g/L$ and $15g/L$, increasing by increments of $3g/L$. The gelatine powder was mixed with distilled water, which was used to mimic CSF with particulate matter.

In the experiment gelatine was used to represent the lymphocytes, monocytes and the albumin for the following reasons: i.) because the gelatine would not go into solution at the temperature range that we operated at, ii.) it was easy to clean between experimental runs and iii.) it was not abrasive, thus, minimising potential damage to the tubing. Water was used represent the CSF because water is close in viscosity [21] and density [22] to CSF.

The volume CSF exiting the shunt system at the end of the time interval was recorded and then converted into a volume flow rate, which was used to determine whether the shunt is blocked. The premise behind this is that the lower the volume flow rate, the greater the chance that the shunt is blocked.

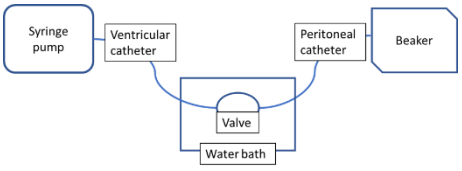

Fig. 4. Test bench schematic

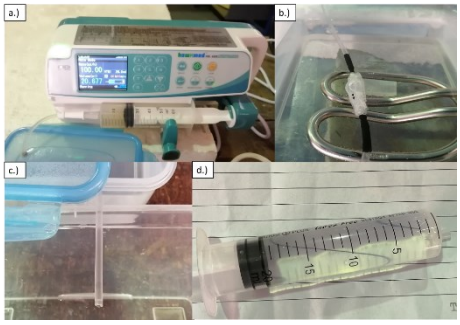

Fig. 5. Experiment

The experiment was carried out in 15-minute intervals per increase in temperature and per increase in concentration. The first readings were taken at $37°C$, then the next readings at $38°C$, $39°C$, $40°C$ and finally $41°C$. The temperature was increased up to $41°C$ as any fever above $41.7°C$ is considered as life-threatening [29]. The shunt valve was immersed in a water bath, with the temperature changed after readings have been taken for each particulate concentration entry. The shunt valve and catheters were flushed out with clean water after every reading to create a fair testing environment. A syringe pump was used to introduce CSF into the mock shunt system. The fluid/particulate mixture at the outlet was collected in a container and was transferred into a syringe with markings for easier reading of the volume. An image of the experimental setup is shown in Fig. 5.

In Fig. 5, image a.) shows the syringe pump with the syringe full of the gelatine mixture. This mixture flowed through the system at the 100ml/hr flow rate. Fig. 5b.) shows the VP shunt valve immersed in the water bath. Fig. 5c.) shows the outlet of the shunt system, where

the fluid/particulate mixture is collected in a container. Fig. 5d.) shows the fluid/particulate mixture collected at the outlet, which was transferred into a syringe to read the volume.

3.2 Experimental results

The volume collected at the outlet at each concentration level and temperature level was plotted on a graph to show the relationship between increasing temperature and volume of the fluid/particulate mixture. The error associated with the results stems from the precision of the measuring instruments used in the experiment [30]. As the smallest graduation of the syringe is $1mL$, the error associated with the measurement of the volume at the outlet is $0.5mL$ [30]. The error bars for the experimental data are also plotted on the graph. Fig. **6** shows the volume of the fluid/particulate mixture at the outlet of the shunt system.

The values obtained for the volume of the fluid/particulate mixture at the outlet of the shunt system are quite accurate for the $6g/L$ and $9g/L$ concentration levels, as the readings are mostly grouped around the $24mL$ mark. This shows that there was little variation in the volume collected at the outlet of the shunt system with increasing temperature. The values obtained at the other concentration levels, i.e., $3g/L$, $12g/L$, and $15g/L$, were more dispersed and therefore less accurate. Therefore, the experiment is repeatable for the two midrange concentration levels, and not the lowest or the highest concentration levels.

The experiment was run as per the setup described in the previous section. The volume flow rates recorded at the outlet are mostly similar to the volume flow rate at the inlet, with some values that fall outside of this range. These results mostly deviate from the original hypothesis, which was that the volume flow rate of the fluid/particulate mixture at the outlet would decrease with increasing concentration and temperature, i.e. the lowest volume flow rate would ideally be found at the $15g/L$ concentration at 41°C. These results show that there is a low chance of shunt occlusion as the decrease in flow rate is not high enough to show that there is significant particulate accumulation in the shunt system.

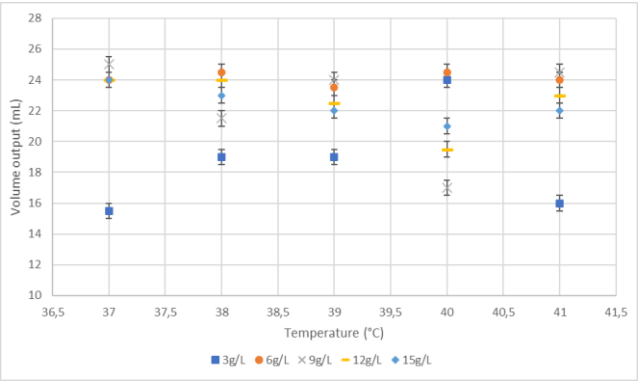

Fig. 6. Volume at the outlet with experimental error

From the data points collected, the conclusion that can be drawn is that the variation in temperature has no effect on the ability of the particles to accumulate along the walls of the shunt system, as each iteration of the results yielded clear fluid at the distal end. This could be attributed to the fact that the gelatine particles sink to the bottom of a container when the fluid is standing. The fluid was regularly agitated throughout the experiment to ensure that the particles do flow through the system, but this made no difference to the concentration of particulates in the fluid at the output. It was found that the particulates would accumulate at

the inlet of the shunt valve, but the particulate accretion did not affect the fluid flow significantly.

The accumulation of particles at the inlet of the shunt system was expected, but the effect which it had on the experiment was not. The assumption made was that the particulate mixture would flow through the system even though there were particles at the inlet of the system. This is analogous to a ventricular catheter being slightly blocked but still allowing fluid with particulates through. However, in this experiment, the particles somewhat filtered the fluid out. The densities of the fluid and the particles are different, but the separation of the two mediums was not considered. This showed that the area of the shunt system that is most prone to blockage is the inlet of the ventricular catheter, as per Tamburrini, Calderelli and Di Rocco [7] but also that the effect of the blockage is minor when the test is run for a short period of time. The serious effect of the blockage may take effect over a long period of time and will only then pose a danger to the health of the patient.

4 CFD Model Results and Discussion

4.1 Validation of CFD model

For the CFD model, the first step that was taken was to validate the model. The model was run at every temperature and particulate concentration, and the volume flow rate at the outlet was recorded.

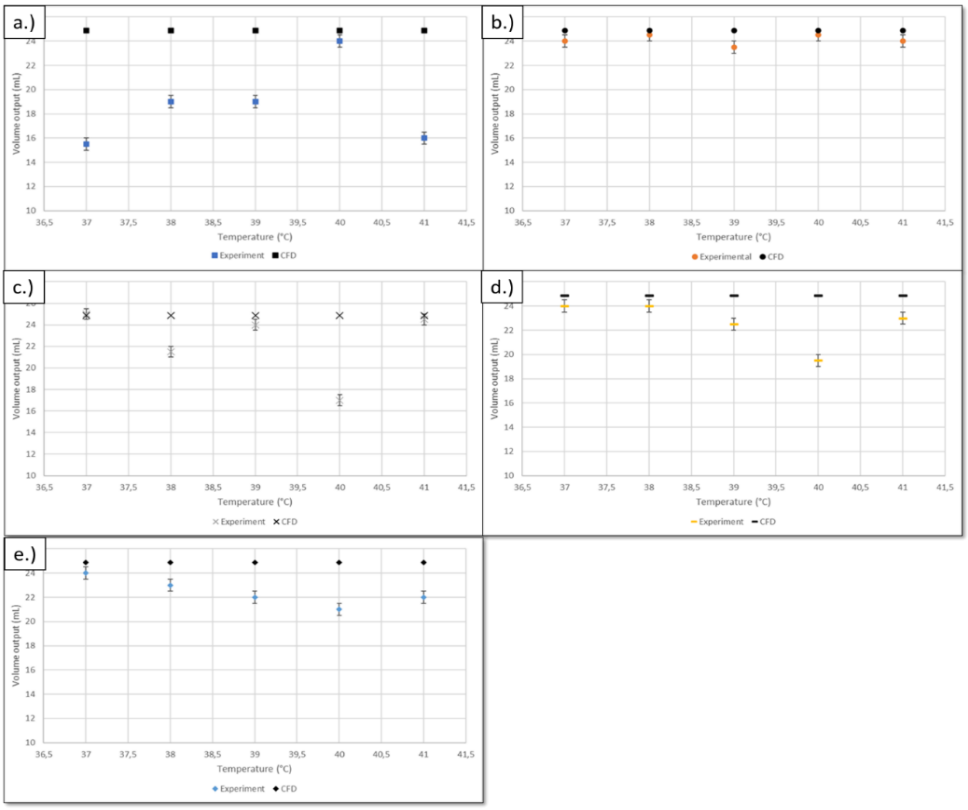

Fig. 7. Graphs of experiment vs CFD for a.) 3g/L, b.) 6 g/L, c.) 9 g/L, d.) 12 g/L and e.) 15 g/L

The volumes obtained at the outlet were compared, as the error due to the measuring instrument for the experiment could be accounted for. As can be seen in Fig. **7**, the graphs for the $6g/L$ and $9g/L$ show that the CFD model is a good approximation of the real behaviour of a VP shunt under the test conditions. The differences between the experimental results and the results of the CFD model are minimal. Some of the readings from the CFD model fall within range of the error bars for the readings that were obtained in the experiment. For the other three concentration levels, the CFD model is not a very good approximation of the shunt behaviour as the differences between the results from the experiment and CFD model differ greatly in some instances. There could have been fewer discrepancies with the experiment for the $6g/L$ and $9g/L$ concentrations compared to the other concentration levels. However, the model is still valid.

The relative error associated with this model can be determined using the following formula:

$$\%\ error = \left|\frac{CFD - experimental}{experimental}\right| * 100 \tag{6}$$

The average relative error associated with the experiment and the CFD model was found to be 15.1%. This average was taken for all the readings based on all the tests that were done. The readings that fall outside of the $23 - 25\ mL$ band resulted in greater error margins, whereas the readings within the band resulted in lower error margins. Taking the error associated with the experimental results into account, the results obtained from the CFD model are comparable with the results from experiment and the model is valid.

4.2 CFD model results

The most definitive method of determining if there is shunt occlusion is by observing the volume flow rate at the outlet in relation to the inlet. The volume flow rate decreased by $0.45ml/hr$ for all cases obtained from the CFD model, which is not a decrease that points towards a definite blockage in the shunt system as this is only 0.45% of the inlet flow rate. The changes in particulate concentration and temperature did not affect the fluid flow at these conditions.

Three locations in the shunt valve have been studies as they are locations where the flow characteristics may change due to geometry and may be points of interest in terms of potential sites for blockage. The flow patterns within the shunt valve are shown using velocity vectors, which are shown in Fig. **8**. The dominant flow is in the positive z-direction, directing the fluid/particulates towards the outlet. The flow has characteristic recirculation zones, as shown in the circled regions in Fig. **8**, near the inlet (Fig. **8**a), upstream and downstream of the void (Fig. **8**b) and near the outlet (Fig. **8**c),. These recirculation regions are potential sites for entrainment, recirculation and accumulation of particles and subsequently potential sites for blockage.

One key observation is that there is a decrease in particulate loading between the inlet and outlet of the model. As shown in Fig. **9,** the particulate loading is largest near the inlet. Considering the large recirculation zones observed near the inlet, as shown in Figure 8a, the inlet is likely the site with the highest probability for blockage.

This was also observed in the experiments, as there were instances where the fluid collected at the outlet of the shunt system contained almost no particulates and that there was an accumulation of particles at the inlet of the shunt. The models that were run had varying results – in the $3g/L$, $12g/L$ and $15g/L$ concentration bands, the maximum DPM concentration at the outlet of the shunt system tended to decrease with increasing temperature but the opposite was true for the $6g/L$ and $9g/L$ concentration bands.

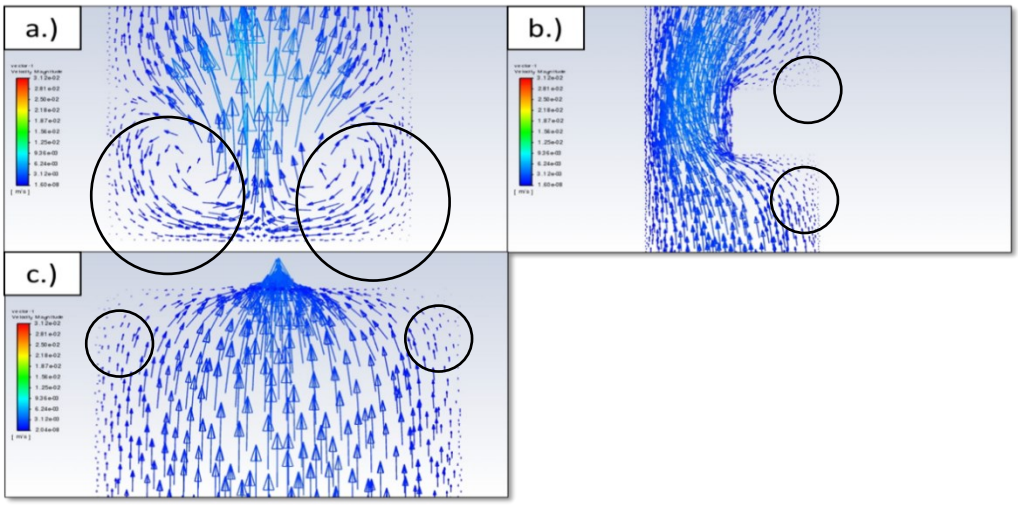

Fig. 8. Velocity vectors for valve inlet (a.), void (b.) and valve outlet (c.)

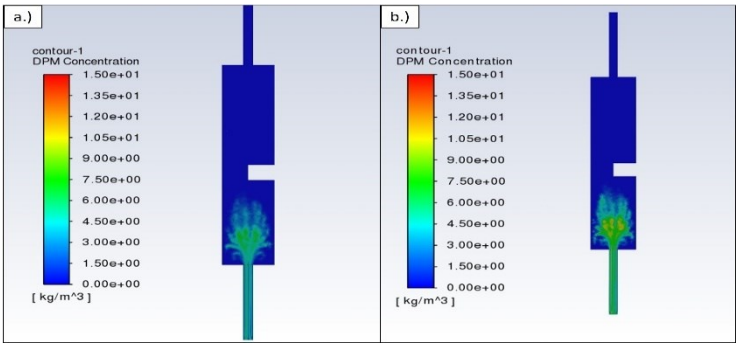

Fig. 9. DPM concentration at valve inlet at 41°C for a.) 6g/L and b.) 9g/L

5 Conclusions

This study investigated whether the occlusion of a shunt valve is accelerated by the presence of an infection using CFD and experiment. The results obtained in the experiment and the CFD model show that there is no real relationship between increasing particulate concentration and temperature, and shunt occlusion at the shunt valve. The general conclusion that could be drawn from the models that were run is that the change in particulate concentration and temperature did not affect the outlet flow rate. This shows that there was no shunt occlusion due to changes in the temperature of the fluid/particulate mixture, as well as the increase in concentration.

The model helped with providing a better understanding of the flow through a VP shunt when the shunt is suspended in an environment with changing temperature, as it effectively showed that increasing temperature and particulate concentration alone do not affect the functionality of the VP shunt system. This result excluded the VP shunt valve as a region of shunt occlusion due to infection, as there would be no bacterial growth in this region. The VP shunt will only malfunction due to infection only when there is a blockage of the proximal or distal catheters [6]. These two regions are more prone to bacterial growth than the shunt valve itself.

These results are valid in as far as the assumption that infection manifests in a.) the change in temperature of the CSF and/or shunt surfaces and b.) an increase in particulates as a consequence of the rise in white blood cells in response to infection. Future work should focus on extending the biological complexity of infection beyond the reductionist assumptions of heat transfer and particulate mechanics. Instead, complexity such as bacterial growth along the shunt surfaces must be modelled to better understand the effect of infection on shunt occlusion. Furthermore, the non-Newtonian behaviour of the fluid in the presence of soluble particles such as albumin should be accounted for in future work.

The Centre for High Performance Computing (CHPC) is acknowledged for the use of the CHPC facilities.

References

1. R. Rizvi, Q. Anjum, *Hydrocephalus in Children*, Journal of Pakistan Medical Association, **55**, 11, (2005)
2. M. Hussain, R. A. Raja, A.-u.-D. Shaikh, M. H. Ali, *Ventriculoperitoneal Shunt Blockage*, Journal of Ayub Medical College, Abbottabad, **24**, (2012)
3. S. Moyle, *Hydrocephalus and Shunts*, Ausmed, 13 April 2017. [Online]. Available: http://www.ausmed.com/articles/hydrocephalus-and-shunts/ [Accessed 7 December 2017]
4. Johns Hopkins University Staff, *Shunt Procedures*, The Johns Hopkins University, The Johns Hopkins Hospital and Johns Hopkins Health System, [Online]. Available: http://hopkinsmedicine.org/neurology_neurosurgery/centers_clinics/cerebral-fluid/procedures/shunts.html [Accessed 7 December 2017]
5. Y. Gutierrez-Murgas, J. N. Snowden, *Ventricular shunt infections: Immunopathogenesis and clinical management*, Journal of Neuroimmunology, **276**, 0, (2014)
6. D. L. Wells, J. M. Allen, Ventriculoperitoneal Shunt Infections in Adult Patients, AACN Advanced Critical Care, **24**, 1, (2013)
7. G. Tamburrini, M. Calderelli,, C. Di Rocco, *Diagnosis and management of shunt complications in the treatment of childhood hydrocephalus*, Reviews in Neurosurgery, **1**, 3, (2002)
8. T. D. Simon, J. Butler, K. B. Whitlock, S. R. Browd, R. Holubkov, J. R. W. Kestle, A. V. Kulkarni, M. Langley, D. D. Limbrick, N. Mayer-Hamblett, M. Tamber, J. C. Wellons, W. E. Whitehead, J. Riva-Cambrin, *Risk Factors for First Cerebrospinal Fluid Shunt Infection: Findings from a Multi-Center Prospective Cohort Study*, The Journal of Pediatrics, **164**, 6, (2014)
9. A. Yilmaz, A. M. Musluman, N. Dalgic, T. Cansever, T. Dalkilic, E. Kundakci, Y. Aydin, *Risk factors for recurrent shunt infections in children*, Journal of Clinical Neuroscience, **19**, (2012)
10. T. Ramokoka, *Modelling fluid and particulate flow through a VP shunt,* University of Johannesburg, Johannesburg, (2017)
11. A. C. Aralar, M. D. Bird, R. D. Graham, B. Koo, M. B. Shenai, P. V. Chitnis, S. Sikdar, *Ultrasound Characterization of Interface Oscillation as a Proxy for Ventriculoperitoneal Shunt Function*, in Proceedings of the 38th Annual International Conference of the IEEE Engineering in Medicine and Biology Society (EMBC), Orlando, (2016)
12. ANSYS Inc., *ANSYS Fluent Meshing User's Guide*, SAS, Inc., Canonsburg, (2016)

13. Autodesk Support, *How to Perform a Mesh Convergence Study*, Autodesk, Inc., 24 May 2015. [Online]. Available: https://knowledge.autodesk.com/support/simulation-mechanical/learn-explore/caas/sfdcarticles/sfdcarticles/How-to-Perform-a-Mesh-Convergence-Study.html [Accessed 23 June 2019]
14. P. J. Roache, *Perspective: A Method for Uniform Reporting of Grid Refinement Studies*, Journal of Fluid Engineering, **116**, (1994)
15. V. Kurtcuoglu, D. Poulikakos, Y. Ventikos, *Computational Modeling of the Mechanical Behaviour of the Cerebrospinal Fluid System*, ASME Journal of Biomedical Engineering, **125**, (2005)
16. Comsol, Inc., *Navier-Stokes Equations*, Comsol, Inc., 22 February 2017. [Online]. Available: https://www.comsol.com/multiphysics/navier-stokes-equations [Accessed 26 September 2019]
17. B. Munson, T. Okiishi, W. Huebsch , A. Rothmayer, *Differential Analysis of Fluid Flow*, in Fundamentals of Fluid Mechanics, Sixth Edition, Singapore, John Wiley & Sons, Inc., pp. 307-308, (2009)
18. ANSYS Inc., *ANSYS Fluent Theory Guide*, SAS IP, Inc., Canonsburg, (2016)
19. Faculty of Biological Sciences, University of Leeds, *White blood cells*, University of Leeds, [Online]. Available: https://www.histology.leeds.ac.uk/blood/blood_wbc.php [Accessed 13 September 2019]
20. A. Tojo, S. Kinugasa, *Mechanisms of Glomerular Albumin Filtration and Tubular Reabsorption*, International Journal of Nephrology, **2012**, (2012)
21. I. Bloomfield, I. Johnston, L. Bilston, *Effects of protein, blood cells and glucose on the viscosity of cerebrospinal fluid*, Pediatric Neurosurgery, **28**, 5, (1998)
22. A. Tajima, H. Nakata, S. Lin, V. Acuff , J. Fenstermacher, *Differences and similarities in albumin and red blood cell flows through cerebral microvessels*, **5**, 2, (1992)
23. C. Kotsalos, J. Latt, B. Chopard, *Bridging the computational gap between mesoscopic and continuum modeling of red blood cells for fully resolved blood flow*, Journal of Computational Physics, **398**, (2019)
24. C. Kotsalos, J. Latt, J. Beny, B. Chopard, *Digital blood in massively parallel CPU/GPU systems for the study of platelet transport*, Interface Focus, **11**, (2021)
25. A. Lui, T. Polis, N. Cicutti, *Densities of cerebrospinal fluid and spinal anaesthetic solutions in surgical patients at body temperature*, Canadian Journal of Anaesthesia, **45**, (1998)
26. D.P. Agamanolis, *Chapter 14: Cerebrospinal Fluid*, NEOMED, August 2016. [Online]. Available: http://neuropathology-web.org/chapter14/chapter14CSF.html [Accessed 24 September 2019]
27. Thermtest Europe, *Thermal Conductivity of Water*, Thermtest Europe, 11 February 2021. [Online]. Available: https://thermtest.se/thermal-conductivity-of-water#:~:text=According%20to% 20 literature1%20the,K%20at%2020%20C2%B0C [Accessed 31 July 2021]
28. AZoM.com, *Silicone Rubber*, AZoNetwork, [Online]. Available: https://www.azom.com/properties.aspx?ArticleID=920 [Accessed 31 July 2021]
29. California Pacific Medical Center, *Caring for Your Child's Fever*, Sutter Health, 2015. [Online]. Available: http://www.cpmc.org/advanced/pediatrics/patients/topics/fever.html [Accessed 27 March 2018].
30. Advanced Instructional Systems, Inc. and the University of North Carolina, *Measurements and Error Analysis*, Advanced Instructional Systems, Inc. and the University of North Carolina, 2011. [Online]. Available: https://www.webassign.net/question_assets/unccolphysmechl1/measurements/manual.html [Accessed 26 February 2020].